Evaluation of Parameters Impacting Drug Susceptibility in Intracellular *Trypanosoma cruzi* Assay Protocols

Gyongseon Yang[1,2], Nakyung Lee[1], Jean-Robert Ioset[3], and Joo Hwan No[1]

Abstract

In order to understand the key parameters influencing drug susceptibility, different *Trypanosoma cruzi* assay protocols were evaluated using a comparative assay design. The assays compared in this study were an image-based intracellular *T. cruzi* assay quantified through an image-mining algorithm and an intracellular assay utilizing a β-galactosidase-expressing *T. cruzi* strain. Thirty-one reference compounds known to exhibit activities against intracellular *T. cruzi* were used as benchmarks. Initial comparison using EC_{50} values from two assays showed a very poor correlation, with an R^2 value of 0.005. Nitroheterocyclics and CYP51 inhibitors were inactive in an image-based assay, but were highly active in a colorimetric assay. In order to identify the differentiating factor, we synchronized the compound–parasite incubation times or the sequential cell and compound seeding schemes between assays, but the correlation remained low. A high correlation ($R^2 = 0.86$) was observed only after both compound incubation time and cell seeding were synchronized between assays. Further analysis of EC_{50} and maximum inhibition values showed that nitroheterocyclics and CYP51 inhibitors exhibit relatively large deviations in activity between experimental protocols routinely used for in vitro intracellular *T. cruzi* assays. These findings suggest that the factors mentioned are critical when designing an intracellular *T. cruzi* assay.

Keywords

Introduction

Chagas disease is a vector-borne, parasite-mediated tropical disease caused by *Trypanosoma cruzi*. Approximately 6–7 million people are infected with *T. cruzi* worldwide, with the highest incidence in Latin America.[1] In recent decades, immigration of Latin Americans to developed countries has brought the infection to nonendemic areas, such as Europe and North America.[2] The clinical manifestation of acute infection is a self-limited, febrile illness resulting in <5% mortality. During the chronic stage, symptoms of cardiac or digestive failure appear, along with higher mortality.[3] Benznidazole and nifurtimox are currently the only available therapeutics for Chagas disease, but they are associated with severe side effects and frequently fail to treat the disease.[4] Safer, efficacious, and orally available drugs are urgently needed. Recently, azole-based antifungals, such as posaconazole, were identified as promising drug candidates that showed outstanding potencies in various in vitro systems.[5] However, posaconazole showed significant treatment failure outcomes compared with benznidazole in a randomized clinical trial involving chronic indeterminate Chagas patients. After benznidazole treatment and an initial apparent clearance of parasitemia, 80% of posaconazole-treated patients relapsed within 10 months. The remaining 20% of patients failed to show sustained

clearance of the parasite at the same endpoint.[6] Failure of azoles in clinical trials not only emptied the Chagas late-stage research and development pipeline, but also raised scientific issues related to a lack of translatability from preclinical testing models to clinical outcomes.[6] This left an accentuated need for novel drug candidates to treat Chagas, and underscored the need to better understand the biology of the assay systems used for compound screening, and in vitro/in vivo activity profiling.

Several assay tools have been developed for screening and identifying potential drugs for the treatment of Chagas

[1]Leishmania Research Laboratory, Institut Pasteur Korea, Seongnam-si, Gyeonggi-do, Republic of Korea
[2]Interdisciplinary Programs of Functional Genomics, Yonsei University, Seoul, Republic of Korea
[3]Drugs for Neglected Diseases *initiative* (DND*i*), Geneva, Switzerland

Corresponding Author:
Joo Hwan No, Leishmania Research Laboratory, Institut Pasteur Korea, Seongnam-si, Gyeonggi-do, Republic of Korea.
Email: joohwan.no@ip-korea.org

disease. Cell-based assays that are used in high-throughput screening (HTS) for drug discovery in Chagas disease are generally classified into colorimetric, fluorometric, or image-based high-content assays.[7] The first colorimetric assay using β-galactosidase-expressing *T. cruzi* was reported in 1996,[8] but more recent versions utilize transgenic parasites that express tdTomato, luciferase,[9] or green fluorescent protein (GFP).[10] These resources can be easily utilized in many laboratories without the need for sophisticated imaging equipment. Leveraging the availability of fluorescent parasites, a series of image-based high-content assays were developed. Together with advances in image-mining software, the identification and quantification of parasites within host cells is now possible. This approach provides much more detailed information than colorimetric assay outputs, including data on parasite numbers, parasite infection ratios (i.e., percentage of host cells infected with parasites), and host cell cytotoxicity.[11] Such a wealth of data makes image-based high-content assays the state-of-the-art technology for high-throughput phenotypic drug screening against intracellular parasites. Hence, a variety of assays that use various host cells and parasites with differing multiplicities of infection (MOIs), experimental setup, and detection approaches have been established. Such approaches are currently employed in many labs worldwide for drug screening and profiling purposes.

We evaluated differences in susceptibility to compounds known to exhibit in vitro activity against *T. cruzi* using a widely established colorimetric assay protocol[8] in order to benchmark our in-house image-based intracellular *T. cruzi* assay.[11] The objectives of this study were to compare compound susceptibilities via the two assay protocols and identify variables within the experimental procedures that may provide different results. This would allow us to better understand the utility of two generations of intracellular *T. cruzi* assays applied to Chagas disease drug discovery.

Material and Methods

Chemicals

A panel of 31 control compounds were selected as benchmarks. It included drugs currently used in the field for the treatment of Chagas disease (benznidazole and nifurtimox), clinical candidates and active metabolites of clinical candidates (posaconazole, ravuconazole, fexinidazole, and fexinidazole sulfone), representative compounds of chemical classes currently under preclinical or clinical development, including nitroimidazoles and oxaboroles, and a few earlier-stage hits reported elsewhere for their in vitro activity against *T. cruzi* intracellular amastigotes. Several of these compounds have been associated with in vivo activity in one or more animal models infected with *T. cruzi*.

Parasites and Cell Culture

Human osteosarcoma cell line U2OS (ATCC HTB-96), rhesus monkey kidney epithelial cell LLC-MK2 (ATCC CCL-7), and skeletal muscle cell line L6 (ATCC CRL-1458) were purchased from the American Type Culture Collection (ATCC). Cells were cultured in Dulbecco's modified Eagle's medium (DMEM) with high-glucose (GIBCO, Grand Island, NY) supplemented with 10% fetal bovine serum (FBS, GIBCO), 100 μ/mL penicillin (GIBCO), and 100 μg/mL streptomycin (GIBCO) at 37 °C in 5% CO_2. LLC-MK2 and L6 cells were used to maintain *T. cruzi* Y and Tulahuen strains in vitro, respectively, while U2OS and L6 cells were used as host cells. Cells were washed with complete media every 48 h after initial infection to remove extracellular metacyclic trypomastigotes (TCTs) and epimastigotes. Tissue culture–derived TCTs were harvested from culture supernatant 7 days after initial infection. TCTs were then used for colorimetric and image-based assays.

Colorimetric Assay

L6 cells were seeded in 384-well μCLEAR plates (Greiner Bio-One, Monroe, NC) at 400 cells in 40 μL of DMEM per well for 24 h and then inoculated with 1320 parasites of TCT *T. cruzi* Tulahuen strain in 10 μL of DMEM (MOI of 1:4). Various compound concentrations were applied 48 h postinfection. After 72 h, CPRG/Nonidet substrate (Sigma, St. Louis, MO) was added to the wells, and plates were further incubated for 2–4 h. Fluorescence emission was measured at 530 nm wavelength using a SpectraMax M5 (Molecular Devices, Sunnyvale, CA). Parasite amounts were quantified based on relative fluorescence intensity. Experiments were performed in duplicate.

Image-Based Assay

Each well of the 384-well μCLEAR plate containing test compound was seeded with 50 μL of a mixture containing 4.0×10^3 U2OS cells and 6.0×10^4 *T. cruzi* Y strain TCTs (MOI of 1:15), in which the master mixture was prepared by 5 min incubation of the host cells and the parasites with gentle swirling. After 48 or 72 h incubation with the test compounds, plates were fixed with 4% paraformaldehyde (Sigma) and washed with phosphate-buffered saline (PBS, GIBCO) to remove external parasites using a BioTek EL402 washer (BioTek Instruments Inc., Winooski, VT). U2OS and parasite DNA were stained with 5 μM DRAQ5 (Biostatus, Shepshed, UK), and fluorescent images were acquired using an Operetta instrument (Perkin Elmer, Hamburg, Germany) at excitation/emission wavelengths of 633/690 nm. Images were analyzed using custom, in-house software.[11] Experiments were performed in duplicate.

Modified Image-Based Assay

Modified image-based assay seeding schemes and MOIs were identical to those used for colorimetric assays, but specific host cell, parasite strain, incubation time, and read-out methods were adapted to the image-based assay protocol. U2OS cells were seeded in 384-well plates at 1.0×10^3 cells per well. After 24 h, cells were inoculated with 4.0×10^3 *T. cruzi* Y strain TCTs per well. Drugs were added to the wells after 48 h infection and incubated at 37 °C for 48 and 72 h. After compound exposure, plates were fixed with 4% paraformaldehyde for 15–30 min, and the cell monolayer was then washed with PBS and stained with 5 μM DRAQ5. Images were acquired and analyzed by the method described above.

Data Analysis

Assay images were analyzed using in-house image-mining software developed for high-content analysis. This software has a built-in *T. cruzi* infection analysis algorithm for quantifying cell number, parasite number, and infection ratio.[11] As positive and negative controls, noninfection and infection in 1% DMSO were used, respectively. The activity was assessed using the infection ratio and relativized to values obtained from positive and negative controls on each plate. Dose–response curves (DRCs) were fitted using Prism (GraphPad, La Jolla, CA). The half-maximal effective concentration (EC_{50}) was determined from the normalized activity dataset fitted curves.

Results and Discussion

Selection of Reference Drugs

A set of 31 reference drugs have been used as benchmarks in the course of this comparative study. This chemically and biologically diverse compound collection (**Fig. 1**) has been selected, based on a variety of criteria detailed below. As a common denominator, all compounds have been previously reported to be active in one or more phenotypic *T. cruzi* intracellular assays. This benchmarking set notably includes nifurtimox and benznidazole as the two nitroheterocyclic drugs currently used to treat Chagas disease in the field. It also contains fexinidazole—and its active metabolite fexinidazole sulfone—a drug currently under evaluation in phase II clinical trials for the treatment of Chagas disease. Antifungals with potent antitrypanosomal activity, including posaconazole,[6] itraconazole, ravuconazole,[12] terconazole,[13] fenarimol, EPL-BS967, and EPL-BS1246,[14] are also included in the test set. The latter two molecules were identified from a lead optimization program initiated on the fungicide fenarimol. These azole- or pyridine-based molecules are known to be potent inhibitors of CYP51 (Sterol 14α-demethylase), an enzyme in the ergosterol biosynthetic pathway[15] of *T. cruzi* parasites, as well as in fungi. Existing treatments for human African trypanosomiasis (HAT), such as pentamidine[16] and eflornithine,[17] as well as visceral leishmaniasis treatments amphotericin B and miltefosine, are included, as they are also known to exhibit *T. cruzi* growth inhibition in vitro. Finally, a dozen *T. cruzi* cell growth inhibitors from various sources are included. The oxaboroles AN10227 and AN4169 were initially found to be active against *Trypanosoma brucei* and further confirmed to be active against *T. cruzi* in vitro, and eventually in vivo in the case of AN4669.[18] Allopurinol,[19] formycin B,[20] fluphenazine,[13] thioridazine,[21] amiodarone,[22] azelastine, clemastine,[23] lonidamine,[24] loperamide,[13] menadione,[25] quinacrine,[26] and tafenoquine[27] are all agents included in the test set because they show some activity against *T. cruzi* growth in vitro.

Comparison of Colorimetric versus Image-Based Assay

The 31 chemicals listed above were used to benchmark and compare the different assay protocols under evaluation. For the colorimetric assay (**Fig. 2A**), L6 host cells were used and the β-galactosidase-expressing *T. cruzi* Tulahuen strain was used for infection. L6 cells were seeded onto assay plates and after 24 h cells were infected with parasites at an MOI of 1:4. The compound treatment occurred at 48 h after infection, followed by 72 h incubation time. Parasite viability was measured by a colorimetric method based on levels of β-galactosidase expression, and this expression of exogenous protein is less likely to contribute to differences in drug susceptibility based on the previous report.[8] U2OS host cells and the *T. cruzi* Y parasite strain were used for the initial image-based assay protocol (**Fig. 2B**). The MOI was 1:15 for the TCT ratio of parasite to host cells, and compounds were added within an hour. After 48 h of infection, cells were fixed and stained with DNA dye, and images were acquired by a high-throughput confocal imager. Images were then analyzed to quantify parasite number, infection ratio, and host cell numbers as previously reported, and the infection ratio was used as a measure of tested compound activity.[11] Compounds were tested across a 10-point, twofold dilution series, and readouts were analyzed to calculate the EC_{50} and maximum inhibition values (Max %) (**Suppl. Table S1**).

We first compared EC_{50} values for the compounds tested generated through colorimetric and image-based assays by plotting pEC_{50} ($= -\log EC_{50}$) values. Based on the linear regression, a very poor correlation of $R^2 = 0.005$ (slope = −0.09; **Fig. 3A**) was observed. Upon analyzing the scatter plot, we noticed that among the 31 compounds tested, 17 were inactive when assessed through the image-based assay, even at highest tested concentrations of 100 or 50 μM, while they were active in the colorimetric assay.
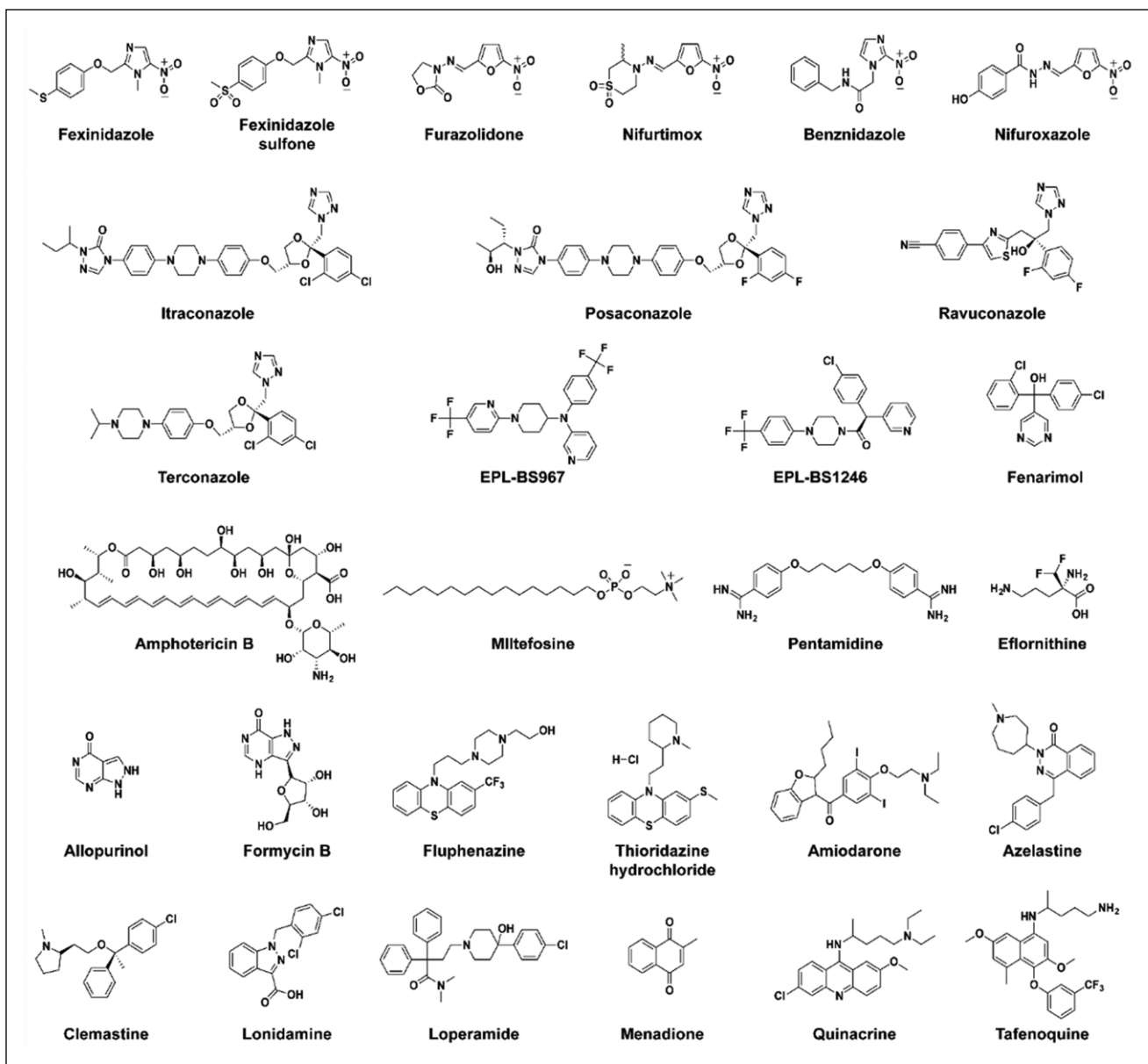
Figure 1. Structures of the compounds used in this study.

Included in these 17 compounds were all the azole-based CYP51 inhibitors (e.g., posaconazole and itraconazole), as well as some nitroheterocyclics (fexinidazole, fexinidazole sulfone, furazolidone, and nifuroxazide), pyrazolopyrimidines (allopurinol and formycin B), amiodrone, and menadione. Remarkably, most of the CYP51 inhibitors showed little activity at 100 μM in the image-based assay, where percentage inhibitions were itraconazole, 2.4%; posaconazole, 11%; ravuconazole, 15%; terconazole, 31%; and fenarimol, 18%. However, in the colorimetric assay these compounds were highly active, giving EC_{50} values of 0.39 μM for itraconazole, 0.038 μM for terconazole, and <0.0051 μM for posaconazole and ravuconazole. Clinically used

Chagas treatments nifurtimox and benzimidazole also showed large variation in potencies (23- and 29-fold difference between assays, respectively).

Two drugs, eflornithine and lonidamine, lacked any inhibition in both assays. Interestingly, the standard of care for visceral leishmaniasis—miltefosine and amphotericin B—exerted relatively higher activity in image-based assays (EC_{50} = 0.58 and 0.41 μM, respectively) than in colorimetric assays (27 and 21 μM, respectively). This difference may possibly be linked to the mode of action of amphotericin B and miltefosine. For an instance in the image-based assay, these compounds could act on the extracellular parasites (TCTs) before the invasion of host or before the
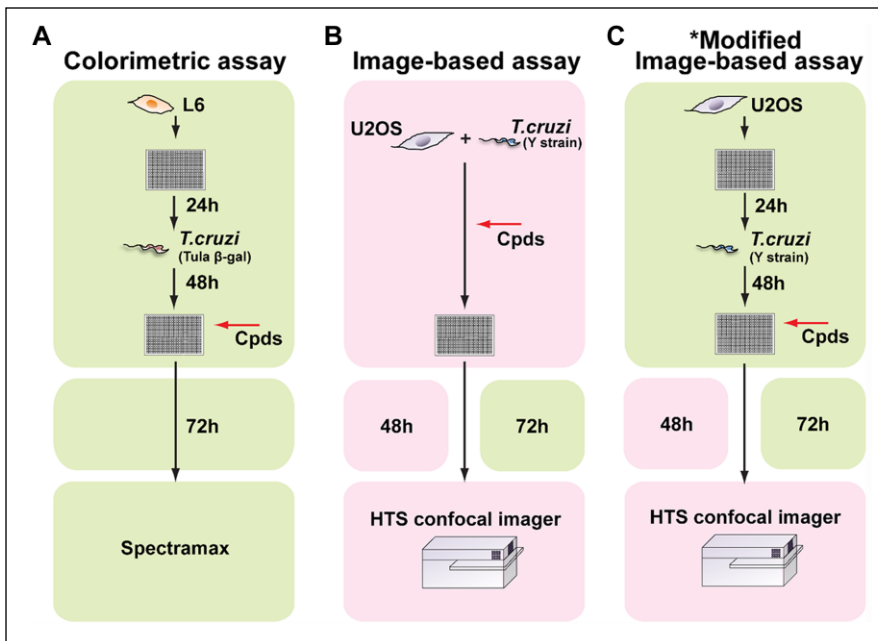
Figure 2. Intracellular *T. cruzi* assay schemes used in this study. A colorimetric assay, using a β-galactosidase-expressing *T. cruzi* Tulahuen strain (L6 cells as host cells), and an image-based assay, using the *T. cruzi* Y strain (U2OS cells as host cells), are illustrated. *Modified image-based assay: Image-based assay with the seeding scheme replaced with that of the colorimetric assay.
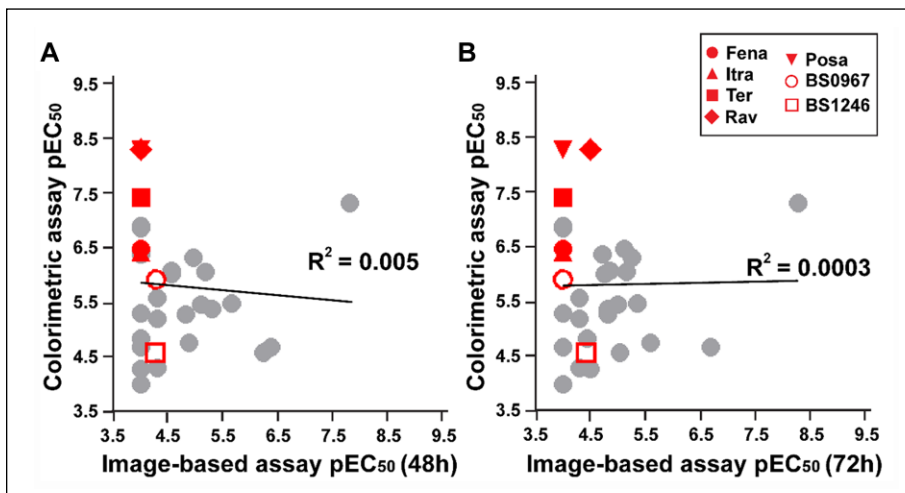

Figure 3. Correlation plots of activity values from colorimetric and image-based assays. (**A**) Correlation between colorimetric and image-based assay results at 48 h incubation. (**B**) Correlation between colorimetric and image-based assay with 72 h incubation.

differentiation to amastigotes, as both the compounds are known to interact with cellular membranes and their related components.[28,29] Especially for amphotericin B, based on its mechanism to bind to ergosterols in membranes, the compound may integrate into the parasite membrane to exert its action while the parasites are outside the host cell. In general, no tight correlation was observed between assays based on compound activity, and EC_{50} values were relatively lower in the colorimetric assays.

Compound Incubation Time and Cell Seeding Schemes

Discrepancies in the inhibitor activity profiles between colorimetric and image-based intracellular *T.* cruzi assays may have resulted from five different variables: host cell type, parasite strain, exposure scheme, compound incubation time, and readout method. Differences in compound activity may also result from multivariable combinatorial effects. Recently, there were investigations into the susceptibilities of nitroheterocyclics and CYP51 in several *T. cruzi* strains.[30] In the study, eight compounds were tested in both *T. cruzi* Y and Tulahuen strains, and using pEC_{50} values, we constructed a scatter plot to measure the correlation and found that the R^2 was 0.97 (analysis not shown). This implied that there were no major differences in parasite strain sensitivity. However, the maximum inhibition of tested compounds changed over the course of the compound–parasite incubation time. Based on this observation, we first increased the incubation time of our image-based assay from 48 to 72 h to
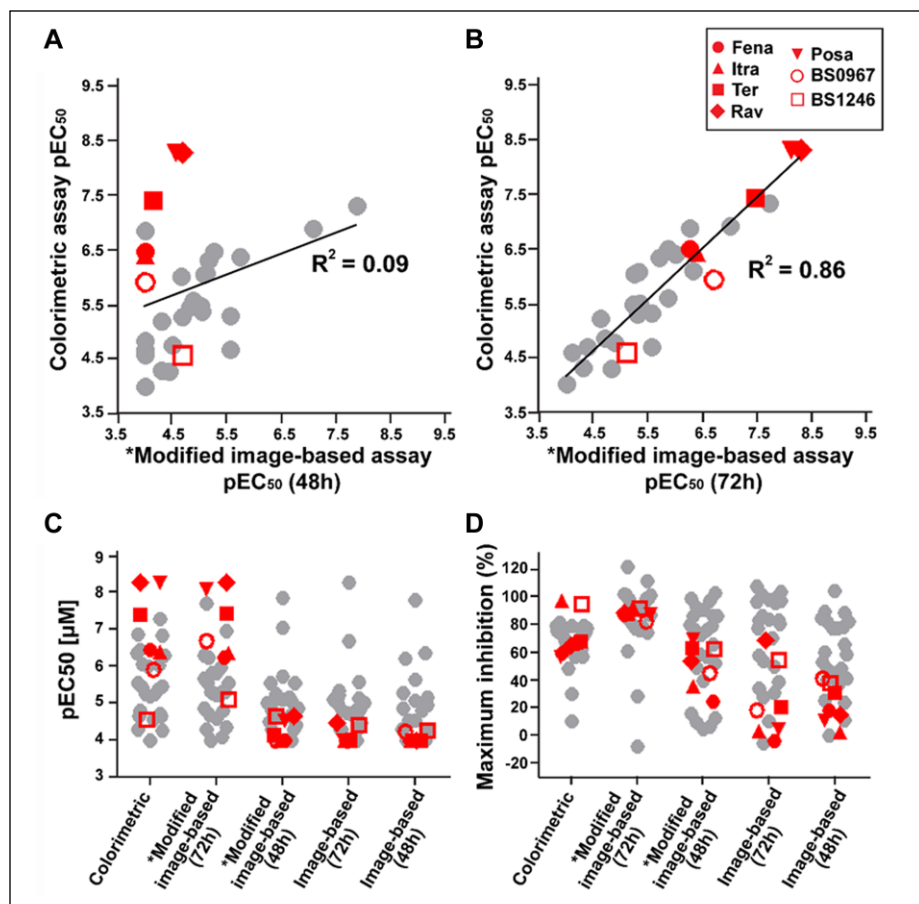
Figure 4. Correlation plots of activity values from colorimetric and modified assays. (**A**) Correlation between colorimetric and modified assay results at 48 h incubation. (**B**) Correlation between colorimetric and modified assay results at 72 h incubation. (**C**) Scatter plots of EC_{50} values from all assays. CYP51 inhibitors are colored red and all the other inhibitors are colored grey. (**D**) Scatter plots of maximum inhibition values. *Modified image-based assay: Image-based assay with the seeding scheme replaced by that of the colorimetric assay.

evaluate potential changes in effectiveness. Most compounds showed similar inhibitory values between 48 and 72 h of incubation, but for nitroheterocyclics, the maximum inhibition increased by 72 h, and EC_{50} values were generated based on a sigmoidal DRC. Respective maximum percentage and EC_{50} values were as follows: fexinidazole, 59% and 37 µM; fexinidazole sulfone, 109% and 32 µM; furazolidone, 99% and 41 µM; and nifuroxazide, 78% and 7.5 µM. Inhibition values for furazolidone and nifuroxazide were still higher from image-based assays than from colorimetric assays, and azoles were not active. Overall, there was no major improvement in correlation between colorimetric and image-based assays with increasing compound incubation time.

Next, we substituted the cells and compound seeding scheme of the image-based assay with those of the colorimetric assay. The host cell (U2OS), parasite (*T. cruzi* Y stain), and compounds were added to the assay plate in a sequential manner with time intervals (**Fig. 2C**). Following this modified image-based assay protocol, compounds were incubated for 48 and 72 h for comparison.

At 48 h compound incubation, results did not match those from the initial colorimetric assay, resulting in an R^2 value of

0.09 (**Fig. 4A**). The main reason for the differences in colorimetric assay outcomes was the low potency of fexinidazole ($EC_{50} > 100$ µM), EPL-BS967 ($EC_{50} > 100$ µM), fenarimol ($EC_{50} > 100$ µM), itraconazole ($EC_{50} > 100$ µM), formycin B ($EC_{50} > 100$ µM), posaconazole ($EC_{50} = 28$ µM), and ravuconazole ($EC_{50} = 21$ µM). In this adapted version of the image-based assay, amphotericin B was inactive while miltefosine activity was retained ($EC_{50} = 2.7$ µM). Even with such differences in potencies, there was a slight increase in efficacy (Max %) for CYP51 and nitroheterocyclics with respect to the original image-based results (**Fig. 4D**).

We then compared the results of the modified, image-based assay after 72 h compound incubation with colorimetric assay results. The correlation dramatically increased, giving an R^2 of 0.86 (**Fig. 4B**). Compounds that showed more than a fivefold difference between tests were limited to benznidazole (6.0×), amphotericin B (40×), miltefosine (7.8×), and quinacrine (5.5×), but most compounds were within a one- to threefold difference between tests. Importantly, both potency and efficacy of CYP51 compounds were very similar for both tests. Several compounds with similar EC_{50} values for the colorimetric and modified phenotypic assays were fenarimol (0.33 µM vs. 0.55 µM),

itraconazole (0.39 vs. 0.42 μM), posaconazole (<0.0051 vs. 0.0077 μM), ravuconazole (<0.0051 vs. <0.0051 μM), and terconazole (0.038 vs. 0.034 μM). The EC_{50} of fexinidazole increased from >100 μM to 20 μM after the extended incubation time, coming close to the values from the colorimetric assay (15 μM). In addition, the EC_{50} of azelastine increased from 13 to 1.4 μM with increased incubation time in the modified image-based assay, reaching a level similar to the colorimetric value of 2.7 μM. Similarly, the EC_{50} of clemastine changed from 7.7 to 0.47 μM with increased time, a value comparable to that from the colorimetric assay (0.85 μM). For efficacy values, the overall maximum percentage of inhibitors reached levels that were similar to those observed in the colorimetric assay (**Fig. 4D**) after extended time, and in particular, CYP51 and nitroheterocyclics achieved almost 100% parasite clearance. Comparing with the previous report by Moraes et al.,[30] the original image-based assay showed a large discrepancy in terms of potency and efficacy for the eight tested compounds, especially with CYP51 inhibitors. However, in the modified version of the image-based assay the values have become similar, except EPL-BS1246, which still had >100 times of difference in the EC_{50} value. This convergence of values is possibly due to the fact that both assays implement a sequential cell and compound seeding scheme, but there still remains minor differences in procedures, such as an extra 24 h of infection time in the modified image-based assay (total of 48 h) and a long compound incubation time of 96 h in the previous report.[30] Nevertheless, it is important to mention that in both assays, nitroheterocyclics, including benzinidazole, nifurtimox, and fexinidazole sulfone, showed 100% maximum inhibition, whereas posaconazole and ravuconazole showed high (80%–90% maximum inhibition) but still incomplete clearance of parasites.

In order to analyze the general trends of potencies, we plotted inhibitor pEC_{50} values derived from all the assay protocols tested. As shown in **Figure 4C**, the image-based assay with 48 and 72 h compound incubation time, as well as the modified version of the image-based assay with 48 h incubation, behaved in a very similar fashion. However, when the modified image-based assay was conducted with 72 h compound incubation, the pEC_{50} values of inhibitors changed dramatically to values similar to those from the colorimetric assay. The maximum inhibition value also followed a pattern similar to that of the pEC_{50} values, but in a more gradual manner (**Fig. 4D**). This result shows that the seeding scheme of the cells and compounds, together with compound incubation time, is a critical factor for the outcome of compound susceptibility in intracellular *T. cruzi* assays. From a biological standpoint, the seeding scheme of the cells and compounds is relevant to the parasite form at which they are exposed to the compounds. In the original image-based assay, the extracellular parasites at the TCT form are exposed to the treated compounds before they

infect the host cells and transform into the amastigote form. However, in the colorimetric and modified versions of the image-based assay, the compounds are treated after 48 h of infection, meaning the compound would have to penetrate the host cell membrane and target the amastigote form of the parasite. And this is one possibility of why differences in compound susceptibility are observed, along with increased compound incubation time. In this study, parasite strains do not play a major role in activity outcome; this is consistent with a previous report.[30]

Inhibition Phenotypes of CYP51 Inhibitors

In the initial image-based assay without any modifications,[11] posaconazole and other CYP51 inhibitors, including itraconazole, ravuconazole, and fenarimol, were not active. This assessment included quantitative measurements that showed high infection ratios for inhibitor-treated parasite-infected hosts. However, on the actual images of posaconazole-treated cells, we observed a dramatic decrease in parasite numbers inside human macrophages compared with controls (**Fig. 5**). This difference between the quantitative values and the visually observed qualitative effect is most likely due to the parameters that we used for activity measurement. In the image-based assay, activity was based on the infection ratio from the image mining process and not on parasite number. This means the hosts harboring a single or few parasites were counted as infected, so even with large decreases of overall parasite numbers, an effective compound could be quantified as inactive. Based on this observation, we compared the activities of the CYP51 inhibitors using two different output parameters from image mining: infection ratio and parasite number. As shown in **Figure 6A**, when the infection ratio (blue line in **Fig. 6A**) is used to generate DRC, the curve is flat and posaconazole is deemed inactive (EC_{50} >100 μM), but once the parasite number (green line in **Fig. 6A**) is incorporated, the DRC shows a sigmoidal curve and an EC_{50} value of 3.0 μM. Similarly, fenarimol gave an EC_{50} value of 32 μM when the parasite number was incorporated. We then generated EC_{50} values for all the CYP51 inhibitors, including azoles and fenarimol analogs, using parasite numbers instead of infection ratio, and further plotted the data to check for a correlation with colorimetric assay values. The slope of linear regression between the colorimetric assay data and the original image-based assay data was −8.12 ($R^2 = 0.62$) after the infection ratio and parasite numbers were incorporated (**Fig. 6B**). Even after changing the parameters from infection ratio to parasite number in the image-based approach, it did not give results that were comparable to those from the colorimetric assays, denoted by a low R^2 of 0.22. On the other hand, the modified image-based method gave slopes of 1.35 ($R^2 = 0.87$) and 1.15 ($R^2 = 0.94$) when the parasite numbers and infection ratios were incorporated, implying an activity trend similar to that observed with the colorimetric assay. With this particular set of CYP51
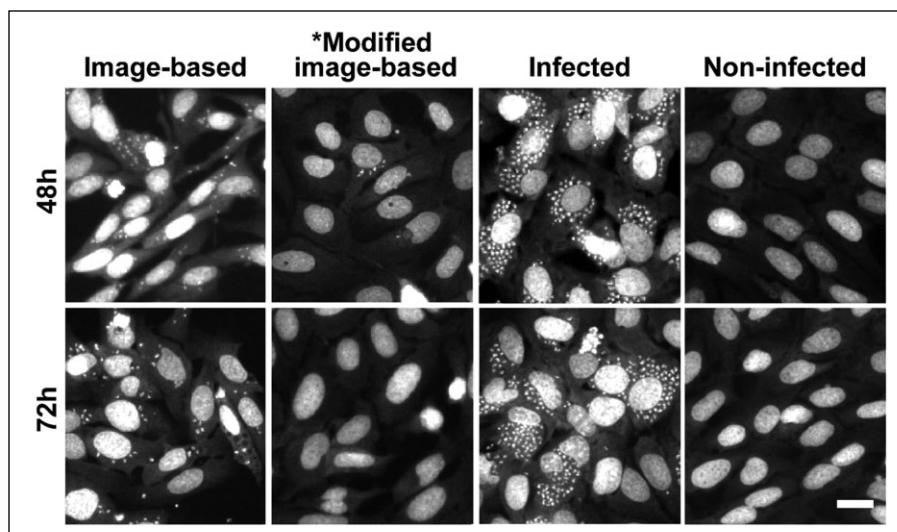
Figure 5. Images from the image-based assay and modified assay for posaconazole treatment at 48 and 72 h at a concentration of 11 µM. Control images of infected and uninfected controls after 48 and 72 h are also shown. Scale bar, 50 µm. *Modified image-based assay: Image-based assay with the seeding scheme replaced with that of the colorimetric assay.
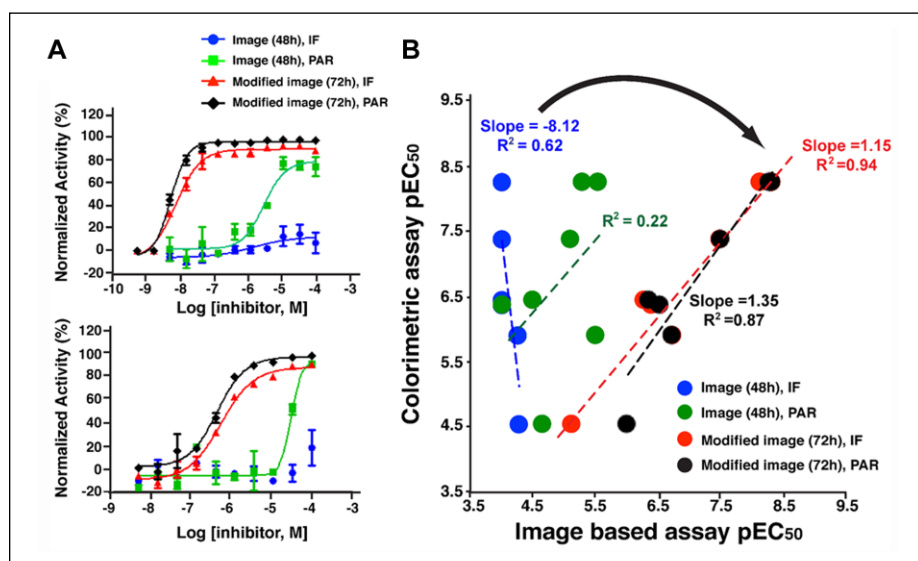

Figure 6. Activity outcomes of CYP51 inhibitors using two different extracted parameters: infection ratio and parasite number. (**A**) DRCs of posaconazole and fenarimol from colorimetric assays and image-based assays (infection ratio and parasite number). (**B**) Change in correlation slope after incorporating infection ratio and parasite numbers. IF, infection ration; PAR, parasite number.

inhibitors, the parameters extracted from the image-based method do not significantly contribute to differences in compound activity.

In order to fully analyze the differences derived from the parameters used in the image-based approach, we have generated scattered plots of infection ratio versus parasite number from all the conducted image-based assays (**Suppl. Table S2**). The initial image-based protocol showed R^2 values of 0.36 and 0.28 for 48 and 72 h of compound incubation, respectively (**Suppl. Fig. S1A,B**). In both assays, AN4169 and formycin B showed nearly a 3 log higher potency when the parasite number was used to generate EC_{50} values, and in general, EC_{50} values were lower when the parasite number was used for the DRC generation. However, in the modified version of the image-based assay,

the EC_{50} values derived from parasite number and infection ratio converged by R^2 values of 0.69 and 0.97 for 48 and 72 h of compound incubation, respectively (**Suppl. Fig. S1C,D**). This implies that in a few cases, such as AN4169 and formycin B, the potency of compounds may depend on the parameter used for the data analysis, but more importantly, this difference is originated from the assay protocol, not from the quantification method itself, since the modified version of the image-based assay (72 h) resulted in almost identical EC_{50} values from parasite number and infection ratio–based analysis. Therefore, in the intracellular *T. cruzi* assay, cell seeding sequence and compound incubation time appear to be the major factors responsible for the observed variation between assays, rather than the choice of parameter used in the image-based protocols.

In summary, we examined the differences between widely used colorimetric and image-based screening assays by evaluating the activities of a set of reference compounds. We found significant variation in compound effectiveness between assays. Discrepancies resulted primarily from cell seeding schemes and compound incubation times. Other factors, such as strain type and readout method, only resulted in minor variations within our experimental setup. Our findings are of general interest to the scientific community investigating Chagas disease drug discovery since they provide insights into the development of intracellular *T. cruzi* assays and interpretation of assay results. These findings also underscore the need for multiple, independent assessments of the activity of potential compounds.

Acknowledgments

Declaration of Conflicting Interests

The authors declared no potential conflicts of interest with respect to the research, authorship, and/or publication of this article.

Funding

References

1. World Health Organization Fact Sheet No. 340. http://www.who.int/mediacentre/factsheets/fs340/en/ (accessed August 2015).

2. Gascon, J.; Bern, C.; Pinazo, M. J. Chagas Disease in Spain, the United States and Other Non-Endemic Countries. *Acta Trop.* **2010**, *115* (1–2), 22–27.

3. Rassi, A., Jr.; Rassi, A.; Marin-Neto, J. A. Chagas Disease. *Lancet* **2010**, *375* (9723), 1388–1402.

4. Viotti, R.; Vigliano, C.; Lococo, B.; et al. Side Effects of Benznidazole as Treatment in Chronic Chagas Disease: Fears and Realities. *Expert Rev. Anti Infect. Ther.* **2009**, *7* (2), 157–163.

5. Goad, L. J.; Berens, R. L.; Marr, J. J.; et al. The Activity of Ketoconazole and Other Azoles against *Trypanosoma cruzi*: Biochemistry and Chemotherapeutic Action In Vitro. *Mol. Biochem. Parasitol.* **1989**, *32* (2–3), 179–189.

6. Molina, I.; Gomez i Prat, J.; Salvador, F.; et al. Randomized Trial of Posaconazole and Benznidazole for Chronic Chagas' Disease. *N. Engl. J. Med.* **2014**, *370* (20), 1899–1908.

7. Bustamante, J. M.; Tarleton, R. L. Methodological Advances in Drug Discovery for Chagas Disease. *Expert Opin. Drug Discov.* **2011**, *6* (6), 653–661.

8. Buckner, F. S.; Verlinde, C. L.; La Flamme, A. C.; et al. Efficient Technique for Screening Drugs for Activity against *Trypanosoma cruzi* Using Parasites Expressing Beta-Galactosidase. *Antimicrob. Agents Chemother.* **1996**, *40* (11), 2592–2597.

9. Canavaci, A. M.; Bustamante, J. M.; Padilla, A. M.; et al. In Vitro and In Vivo High-Throughput Assays for the Testing of Anti-*Trypanosoma cruzi* Compounds. *PLoS Negl. Trop. Dis.* **2010**, *4* (7), e740.

10. Kessler, R. L.; Gradia, D. F.; Pontello Rampazzo Rde, C.; et al. Stage-Regulated GFP Expression in *Trypanosoma cruzi*: Applications from Host-Parasite Interactions to Drug Screening. *PLoS One* **2013**, *8* (6), e67441.

11. Moon, S.; Siqueira-Neto, J. L.; Moraes, C. B.; et al. An Image-Based Algorithm for Precise and Accurate High Throughput Assessment of Drug Activity against the Human Parasite *Trypanosoma cruzi. PLoS One* **2014**, *9* (2), e87188.

12. Urbina, J. A.; Payares, G.; Sanoja, C.; et al. In Vitro and In Vivo Activities of Ravuconazole on *Trypanosoma cruzi*, the Causative Agent of Chagas Disease. *Int. J. Antimicrob. Agents* **2003**, *21* (1), 27–38.

13. Engel, J. C.; Ang, K. K.; Chen, S.; et al. Image-Based High-Throughput Drug Screening Targeting the Intracellular Stage of *Trypanosoma cruzi*, the Agent of Chagas' Disease. *Antimicrob. Agents Chemother.* **2010**, *54* (8), 3326–3334.

14. Keenan, M.; Abbott, M. J.; Alexander, P. W.; et al. Analogues of Fenarimol Are Potent Inhibitors of *Trypanosoma cruzi* and Are Efficacious in a Murine Model of Chagas Disease. *J. Med. Chem.* **2012**, *55* (9), 4189–4204.

15. Buckner, F. S. Sterol 14-Demethylase Inhibitors for *Trypanosoma cruzi* Infections. *Adv. Exp. Med. Biol.* **2008**, *625*, 61–80.

16. Diaz, M. V.; Miranda, M. R.; Campos-Estrada, C.; et al. Pentamidine Exerts In Vitro and In Vivo Anti *Trypanosoma cruzi* Activity and Inhibits the Polyamine Transport in *Trypanosoma cruzi. Acta Trop.* **2014**, *134*, 1–9.

17. Schwarcz de Tarlovsky, M. N.; Hernandez, S. M.; Bedoya, A. M.; et al. Polyamines in *Trypanosoma cruzi. Biochem. Mol. Biol. Int.* **1993**, *30* (3), 547–558.

18. Jacobs, R. T.; Nare, B.; Wring, S. A.; et al. SCYX-7158, an Orally-Active Benzoxaborole for the Treatment of Stage 2 Human African Trypanosomiasis. *PLoS Negl. Trop. Dis.* **2011**, *5* (6), e1151.

19. Marr, J. J.; Berens, R. L.; Nelson, D. J. Antitrypanosomal Effect of Allopurinol: Conversion In Vivo to Aminopyrazolopyrimidine Nucleotides by *Trypanosoma curzi. Science* **1978**, *201* (4360), 1018–1020.

20. Rainey, P.; Garrett, C. E.; Santi, D. V. The Metabolism and Cytotoxic Effects of Formycin B in *Trypanosoma cruzi. Biochem. Pharmacol.* **1983**, *32* (4), 749–752.

21. Paglini-Oliva, P.; Fernandez, A. R.; Fretes, R.; et al. Structural, Ultrastructural Studies and Evolution of *Trypanosoma cruzi*-Infected Mice Treated with Thioridazine. *Exp. Mol. Pathol.* **1998**, *65* (2), 78–86.

22. Benaim, G.; Sanders, J. M.; Garcia-Marchan, Y.; et al. Amiodarone Has Intrinsic Anti-*Trypanosoma cruzi* Activity and Acts Synergistically with Posaconazole. *J. Med. Chem.* **2006**, *49* (3), 892–899.

23. De Rycker, M.; Thomas, J.; Riley, J.; et al. Identification of Trypanocidal Activity for Known Clinical Compounds Using a New *Trypanosoma cruzi* Hit-Discovery Screening Cascade. *PLoS Negl. Trop. Dis.* **2016**, *10* (4), e0004584.

24. Turrens, J. F. Inhibitory Action of the Antitumor Agent Lonidamine on Mitochondrial Respiration of *Trypanosoma cruzi* and *T. brucei. Mol. Biochem. Parasitol.* **1986**, *20* (3), 237–241.

25. Lopetegui, R.; Sosa Miatello, C. [Inhibitory Effect of the Blood on the Lethal Anticrithidia *Trypanosoma cruzi* Activity of Menadione In Vitro]. *Rev. Soc. Argent. Biol.* **1961**, *37*, 134–140.

26. Gamage, S. A.; Figgitt, D. P.; Wojcik, S. J.; et al. Structure-Activity Relationships for the Antileishmanial and Antitrypanosomal Activities of 1′-Substituted 9-Anilinoacridines. *J. Med. Chem.* **1997**, *40* (16), 2634–2642.

27. Yardley, V.; Gamarro, F.; Croft, S. L. Antileishmanial and Antitrypanosomal Activities of the 8-Aminoquinoline Tafenoquine. *Antimicrob. Agents Chemother.* **2010**, *54* (12), 5356–5358.

28. Kaminski, D. M. Recent Progress in the Study of the Interactions of Amphotericin B with Cholesterol and Ergosterol in Lipid Environments. *Eur. Biophys. J.* **2014**, *43* (10–11), 453–467.

29. Barratt, G.; Saint-Pierre-Chazalet, M.; Loiseau, P. M. Cellular Transport and Lipid Interactions of Miltefosine. *Curr. Drug Metab.* **2009**, *10* (3), 247–255.

30. Moraes, C. B.; Giardini, M. A.; Kim, H.; et al. Nitroheterocyclic Compounds Are More Efficacious than CYP51 Inhibitors against *Trypanosoma cruzi*: Implications for Chagas Disease Drug Discovery and Development. *Sci. Rep.* **2014**, *4*, 4703.